Journal of Statistical Mechanics: Theory and Experiment
An IOP and SISSA journal

PAPER: Classical statistical mechanics, equilibrium and non-equilibrium

Ergodic properties of occupation times in heterogeneous media

V Méndez* **and R Flaquer-Galmés**

Grup de Física Estadística, Departament de Física. Facultat de Ciències, Universitat Autònoma de Barcelona, 08193 Barcelona, Spain
E-mail: vicenc.mendez@uab.cat

Received 17 November 2025
Accepted for publication 28 December 2025
Published 20 January 2026

Online at stacks.iop.org/JSTAT/2026/013203
https://doi.org/10.1088/1742-5468/ae337d

Abstract. We investigate the ergodic properties of Brownian motion in heterogeneous media through the statistics of occupation times. Using the Feynman–Kac formalism, we derive analytical expressions for the distributions, moments, and ergodicity-breaking parameters of occupation times in two models with spatially varying diffusion coefficient: a piecewise-constant profile and a power-law profile. In the piecewise model, the half occupation time and the occupation time within an interval follow asymmetric arcsine and half-Gaussian distributions, respectively, indicating non-ergodic behavior. For the power-law case, the corresponding distributions are the Lamperti and Mittag–Leffler. In both models, we identify a transition from non-ergodic to ergodic dynamics as the exponent vary. Numerical simulations fully corroborate the analytical results, demonstrating the effectiveness of the Feynman–Kac approach for quantifying ergodicity in heterogeneous diffusion processes.

Keywords: ergodicity breaking, stochastic processes, Brownian motion

*Author to whom any correspondence should be addressed.

© 2026 IOP Publishing Ltd and SISSA Medialab srl. All rights, including for text and data mining, AI training, and similar technologies, are reserved.

Contents

1. Introduction

Heterogeneous diffusion processes have received growing attention in recent years, motivated by the need to understand transport in complex systems where microscopic properties vary in space or time. Such systems arise naturally in physics, chemistry, and biology, encompassing transport in porous materials, colloidal suspensions, and intracellular environments. The nonuniform structure of these media often induces strong spatial dependencies in local transport coefficients, leading to diffusion dynamics that deviate significantly from classical Brownian motion. Studies of diffusion in heterogeneous media cover a wide range of scenarios, including particles confined between nearly parallel plates [1], diffusion under temperature gradients [2], nanoporous solids [3], and confined hard-sphere fluids [4]. In parallel, experimental developments–particularly single-particle tracking techniques [5–11]-have enabled the direct observation of individual trajectories, uncovering pronounced spatial variations of the diffusion coefficient. For instance, both experimental and numerical investigations have shown that the diffusion coefficient of proteins within the cell cytoplasm depends systematically on position

J. Stat. Mech. (2026) 013203

[12, 13]. These results highlight the importance of accounting for space-dependent diffusion coefficient in realistic descriptions of transport.

Models with space-dependent diffusion coefficients have been used successfully in several contexts, such as Richardson diffusion in turbulence [14], mesoscopic transport in disordered porous media [15], and diffusion on random fractal structures [16]. The inclusion of spatial heterogeneity leads to rich and often anomalous dynamical behavior. Recent theoretical analyses have reported phenomena such as non-Gaussian propagators, anomalous scaling of the mean-squared displacement (MSD), and weak ergodicity breaking between time-averaged and ensemble-averaged MSDs [5, 6, 17, 18]. These observations have established heterogeneous diffusion as a minimal and versatile framework for studying deviations from standard ergodic diffusion.

However, most previous studies have characterized ergodicity breaking through ensemble- and time-averaged MSDs, while less attention has been devoted to the complementary perspective based on occupation times-the fraction of time a particle spends in a given spatial region. Occupation-time statistics provide an alternative probe of dynamical sampling and ergodic properties, particularly in systems where the diffusion coefficient varies spatially. They offer a direct measure of how the particle explores distinct regions of heterogeneous space and thus encode information inaccessible from MSD-based analysis alone.

In this work, we investigate the statistical properties and ergodic behavior of a Brownian particle diffusing in heterogeneous media, focusing on the distribution and moments of occupation times. Using the Feynman–Kac formalism, we derive exact and asymptotic results for two classes of functionals: the half occupation time (the time spent by the particle in the positive half-space) and the occupation time within a finite interval. We consider two representative spatial dependencies of the diffusion coefficient: (i) a piecewise-constant dependence, where the diffusion coefficient differs between the positive and negative halves of space, and (ii) a power-law dependence. From the Feynman–Kac equation, we derive the ergodicity-breaking (EB) parameter in terms of the first two moments of the occupation time, and examine its dependence on the form of the spatial heterogeneity. The results elucidate how variations in the diffusion coefficient give rise to nontrivial statistics of occupation times, thereby contributing to a more complete theoretical understanding of anomalous transport and ergodicity breaking in heterogeneous media. While in this work we focus on these two explicit cases, the formalism is general, and can be applied to any other explicit expression for the diffusion coefficient.

Our results are organized as follows. In section 2, we show the Feynman–Kac equation for the characteristic function of a functional of a Brownian particle with a space-dependent diffusion coefficient. We also introduce the two explicit expressions for the diffusion coefficient analyzed in this paper. In section 3, we illustrate how to analyze the ergodic properties from the first two moments of a functional. In sections 4 and 5 we obtain the results for the occupation times in the half space and in an interval, respectively. We conclude in section 6.

J. Stat. Mech. (2026) 013203

2. Generating function of a Brownian functional

Consider the stochastic functional

$$Z\left(t|x_0\right)=\int_0^t U\left[x\left(\tau\right)\right]\mathrm{d}\tau \tag{1}$$

where $U[x(\tau)]$ is a positive function of the stochastic trajectory $\{x(\tau);0\leqslant\tau\leqslant t\}$ of a particle which is initially at x_0, this is, $x(t=0)=x_0$. Let $P(Z,t|x_0)$ be the probability density function (PDF) of the functional $Z(t)$ and $Q(p,t|x_0)$ its characteristic function or generating function, this is,

$$Q\left(p,t|x_0\right)=\int_0^\infty \mathrm{e}^{-pZ}P\left(Z,t|x_0\right)\mathrm{d}Z=\left\langle \mathrm{e}^{-pZ(t)}\right\rangle=\left\langle \mathrm{e}^{-p\int_0^t U[x(\tau)]d\tau}\right\rangle \tag{2}$$

which is nothing but the Laplace transform with respect to Z. Expanding the exponential in power series

$$Q\left(p,t|x_0\right)=\left\langle\sum_{n=0}^\infty\frac{(-p)^n}{n!}Z\left(t|x_0\right)^n\right\rangle=\sum_{n=0}^\infty\frac{(-p)^n}{n!}\left\langle Z\left(t|x_0\right)^n\right\rangle. \tag{3}$$

We also introduce another Laplace transform conjugate to time as

$$\tilde{Q}\left(p,s|x_0\right)=\mathcal{L}_{t\to s}\left[Q\left(p,t|x_0\right)\right]=\int_0^\infty \mathrm{d}t\ \mathrm{e}^{-st}Q\left(p,t|x_0\right). \tag{4}$$

The moments of $Z(t|x_0)$ can be obtained from the derivatives of $\tilde{Q}(p,s|x_0)$ in a systematic manner. To do this, we first define the Laplace transform of the moments

$$\begin{aligned}\left\langle Z\left(s|x_0\right)^n\right\rangle&\equiv\mathcal{L}_{t\to s}\left[\left\langle Z\left(t|x_0\right)^n\right\rangle\right]\\&=\int_0^\infty \mathrm{d}t\ \mathrm{e}^{-st}\int_0^\infty Z\left(t|x_0\right)^n P\left(Z,t|x_0\right)\mathrm{d}Z.\end{aligned} \tag{5}$$

From (2) it is straightforward to show that the moments are represented in terms of the generating function in the following way

$$\left\langle Z\left(s|x_0\right)^n\right\rangle=(-1)^n\left.\frac{\partial^n\tilde{Q}\left(p,s|x_0\right)}{\partial p^n}\right|_{p=0}. \tag{6}$$

Now we need to find the expression for the generating function $\tilde{Q}(p,s|x_0)$ which depends of the details of the underlying random walk. Let $x(t)$ be the position of a Brownian particle moving in a one-dimensional heterogeneous media. It is a stochastic process evolving according the overdamped Langevin equation with a space-dependent diffusion coefficient, namely,

$$\frac{\mathrm{d}x\left(t\right)}{\mathrm{d}t}=\sqrt{2D\left(x\right)}\xi\left(t\right) \tag{7}$$

J. Stat. Mech. (2026) 013203

where $\xi(t)$ is a Gaussian noise with zero mean and autocorrelation $\langle \xi(t)\xi(t')\rangle = \delta(t-t')$. To completely define the meaning of equation (7), we must identify the integral stochastic interpretation adopted. The ergodic properties of the trajectories emerging from equation (7) for different interpretations have been studied in reference [19]. In the following we consider the Langevin equation in the Itô interpretation [20]. The solution to the corresponding Fokker-Planck equation has been found for a variety of examples of $D(x)$ [21, 22]. Such spatially dependent diffusion coefficients model many processes, where a partial list includes random walks in an inhomogeneous medium [1, 23, 24], chemical reactions [25], diffusion (in momentum space) in laser cooling processes [26], dissipative particle dynamics [27], vortex-antivortex annihilations [28], biophysics [12, 29, 30] e.g. measurements of proteins' diffusivity in mammalian cells [12], and modeling of $1/f$ noise [31].

When the particle's position evolves according to (7), the generating function $\tilde{Q}(p,s|x_0)$ of the functional (1) obeys the so called backward Feynman–Kac equation [32]

$$\frac{\partial Q\left(p,t|x_0\right)}{\partial t} = D\left(x_0\right)\frac{\partial^2 Q\left(p,t|x_0\right)}{\partial x_0^2} - pU\left(x_0\right)Q\left(p,t|x_0\right). \tag{8}$$

It is important to note that the expression for the Feynman–Kac equation depends on the stochastic interpretation chosen, and so do all the results obtained from it. For each explicit expression of $U(x)$, we have to solve equation (8) for the generating function using suitable boundary conditions, and then use equation (6) to derive the moments. To do this we need also to specify the explicit expressions for $D(x)$. First we assume the power law dependence [6, 18, 19, 33–35]

$$D\left(x\right) = D_0|x|^{\alpha}, \quad \alpha < 2. \tag{9}$$

The corresponding Fokker-Planck equation for $P(x,t)$ in the Itô interpretation is

$$\frac{\partial P\left(x,t\right)}{\partial t} = D_0\frac{\partial^2}{\partial x^2}\left[|x|^{\alpha}P\left(x,t\right)\right]$$

whose solution is (see appendix C in reference [18])

$$P\left(x,t\right) = \frac{N}{|x|^{\alpha}t^{\frac{1-\alpha}{2-\alpha}}}\mathrm{e}^{-\frac{|x|^{2-\alpha}}{4D_0(2-\alpha)t}} \tag{10}$$

where

$$N = \frac{(2-\alpha)^{\frac{\alpha}{2-\alpha}}}{2D_0^{\frac{1-\alpha}{2-\alpha}}\Gamma\left(\frac{1-\alpha}{2-\alpha}\right)}.$$

The MSD becomes

$$\left\langle x^2\left(t\right)\right\rangle = \int_{-\infty}^{\infty} x^2 P\left(x,t\right)\mathrm{d}x = \frac{2N}{2-\alpha}\Gamma\left(\frac{3-\alpha}{2-\alpha}\right)\left[4D_0\left(2-\alpha\right)\right]^{\frac{3-\alpha}{2-\alpha}}t^{\frac{2}{2-\alpha}}. \tag{11}$$

J. Stat. Mech. (2026) 013203

The diffusion is normal for $\alpha=0$ and ballistic for $\alpha=1$. The subdiffusive regime is found for $\alpha<0$ the superdiffusive for $0<\alpha<1$ and the super-ballistic for $1<\alpha<2$. In simulations, we need to regularize the diffusion coefficient by considering

$$D(x)=\begin{cases} D_0\left(|x|^{\alpha}+\epsilon\right), & \alpha>0 \\ \frac{D_0}{|x|^{-\alpha}+\epsilon}, & \alpha<0 \end{cases}$$

with $\epsilon \ll 1$ to prevent the particles from trapping or divergences at $x=0$ [5, 36].

Another interesting choice for the spatial dependence of the diffusion coefficient is the piecewise constant spatial form [37–39]

$$D(x)=\begin{cases} D_-, & x<0 \\ D_+, & x>0 \end{cases} \tag{12}$$

with $D_\pm>0$. This form of position-dependent diffusion coefficient was previously used to find the solution of the Langevin equation in an open system, without a trapping potential [38]. The MSD in this case is $\left\langle x^2(t)\right\rangle = 2\sqrt{D_+D_-}t$ so that it is diffusive [38].

Below, we illustrate how to compute the generating function and the two first moments for specific functionals. Let us first show how to analyze ergodic properties in terms of the two first moment of a functional.

3. Ergodicity breaking

Let us consider a stochastic trajectory $x(\tau)$ observed from $\tau=0$ up to time $\tau=t$. Consider an observable $\mathcal{O}[x(\tau)]$, a function of the trajectory $x(\tau)$. Since $x(\tau)$ is stochastic in nature, the observable $\mathcal{O}[x(\tau)]$ will also be fluctuating between the realizations. An observable of the random walk is said to be ergodic if the ensemble average equals the time average $\langle\mathcal{O}\rangle=\overline{\mathcal{O}}$ in the long time limit. This means that if $\mathcal{O}[x(\tau)]$ is ergodic then its time average $\overline{\mathcal{O}}$ is not a random variable. As a consequence, the limiting PDF of $\overline{\mathcal{O}}$ is

$$P\left(\overline{\mathcal{O}},t\to\infty\right)=\delta\left(\overline{\mathcal{O}}-\left\langle\overline{\mathcal{O}}\right\rangle\right). \tag{13}$$

At this point, let us define the density $P(x,t)$ which is the probability to find the particle at the point x at time t, i.e. it is the propagator. If the observable is integrable with respect to the density $P(x,t)$, then the ensemble average is

$$\langle\mathcal{O}\left[x\left(t\right)\right]\rangle=\int_{-\infty}^{\infty}\mathcal{O}\left[x\right]P\left(x,t\right)\mathrm{d}x. \tag{14}$$

The time average of $\mathcal{O}[x(t)]$ is defined as

$$\overline{\mathcal{O}\left[x\left(t\right)\right]}=\frac{1}{t}\int_0^t\mathcal{O}\left[x\left(\tau\right)\right]\mathrm{d}\tau. \tag{15}$$

J. Stat. Mech. (2026) 013203

For non-ergodic observables, since $\overline{\mathcal{O}}$ is random, its variance $\mathrm{Var}(\overline{\mathcal{O}})$ is non-zero in the long time limit. Otherwise, for an ergodic observable $\mathrm{Var}(\overline{\mathcal{O}}) = 0$ in the long time limit. Keeping this in mind, one can define the ergodicity breaking parameter EB in the following way

$$\mathrm{EB} = \lim_{t\to\infty} \frac{\mathrm{Var}\left(\overline{\mathcal{O}}\right)}{\left\langle \overline{\mathcal{O}} \right\rangle^2} = \lim_{t\to\infty} \frac{\left\langle \overline{\mathcal{O}}^2 \right\rangle - \left\langle \overline{\mathcal{O}} \right\rangle^2}{\left\langle \overline{\mathcal{O}} \right\rangle^2}. \tag{16}$$

For ergodic observables, one should have $\mathrm{EB} = 0$.

In the examples below we consider the observable $\mathcal{O}[x(t)] = U[x(t)]$ so that the time average of the observable is from (15)

$$\overline{\mathcal{O}\left[x\left(t\right)\right]} = \frac{1}{t}\int_0^t U\left[x\left(\tau\right)\right] \mathrm{d}\tau = \frac{Z\left(t\right)}{t}. \tag{17}$$

and so

$$\left\langle \overline{\mathcal{O}} \right\rangle = \frac{\left\langle Z\left(t\right)\right\rangle}{t}, \quad \left\langle \overline{\mathcal{O}}^2 \right\rangle = \frac{\left\langle Z\left(t\right)^2\right\rangle}{t^2}. \tag{18}$$

Finally, from (16) we can find the ergodicity breaking parameter in terms of the two first moments of the functional

$$\mathrm{EB} = \frac{\left\langle Z\left(t\right)^2\right\rangle}{\left\langle Z\left(t\right)\right\rangle^2} - 1 \tag{19}$$

as $t \to \infty$.

Another quantity of interest which characterizes ergodicity is the PDF of the time averaged observable $\overline{\mathcal{O}[x(t)]}$ around its mean for long times, so we define the dimensionless random variable

$$\eta = \lim_{t\to\infty} \frac{\overline{\mathcal{O}}}{\left\langle \overline{\mathcal{O}} \right\rangle} \tag{20}$$

and from (17) and (18), the relative time averaged observable $U[x(t)]$ is defined by

$$\eta = \lim_{t\to\infty} \frac{Z\left(t\right)}{\left\langle Z\left(t\right)\right\rangle}. \tag{21}$$

Once $P(Z,t|0)$ is found by solving the Feynman–Kac equation (8), the PDF of η follows from

$$P\left(\eta\right) = P\left(Z = \eta\left\langle Z\left(t\right)\right\rangle, t\right)\left\langle Z\left(t\right)\right\rangle. \tag{22}$$

J. Stat. Mech. (2026) 013203

It is interesting to note that the variance of η is nothing but the ergodicity breaking parameter:

$$\mathrm{Var}\,(\eta) = \langle \eta^2 \rangle - \langle \eta \rangle^2 = \langle \eta^2 \rangle - 1 = \frac{\left\langle Z\,(t)^2 \right\rangle}{\langle Z\,(t) \rangle^2} - 1 = \mathrm{EB}.$$

Therefore, for ergodic observables (EB = 0) one has

$$P\,(\eta) = \delta\,(\eta - 1)\,, \tag{23}$$

in agreement with (13).

4. Half occupation time

We consider the occupation time $T^+(t|x_0)$ of the particle above the origin (i.e. on the positive half-space) within a time window of size t if it was at $x = x_0$ at $t = 0$. It is defined as

$$\left\langle T^+\,(t) \right\rangle = \int_0^t \theta\,[x\,(\tau)]\,\mathrm{d}\tau$$

so that $U(x_0) = \theta(x_0)$ in this case. The characteristic function of T^+ has to be solved under the appropriate boundary conditions [40]. If the starting point $x_0 \to +\infty$ the particle will stay on the positive side with $x(t) > 0$ for all finite t implying $T^+(t|x_0 \to +\infty) = t$ and accordingly $P(T^+, t|x_0 \to +\infty) = \delta(T^+ - t)$, i.e. $\tilde{Q}(p, s|x_0 \to +\infty) = 1/(s + p)$. On the other hand, if the starting point $x_0 \to -\infty$ the particle will never reach the positive side and it will stay on the negative half-space implying $T^+(t|x_0 \to -\infty) = 0$ and hence $P(T^+, t|x_0 \to -\infty) = \delta(T^+)$, so that $\tilde{Q}(p, s|x_0 \to -\infty) = 1/s$. Performing the Laplace transform of (8) with respect to t, the Feynman–Kac equation for the characteristic function $\tilde{Q}(p, s|x_0)$ reads

$$s\tilde{Q}\,(p, s|x_0) - 1 = D\,(x_0)\,\frac{\mathrm{d}^2\tilde{Q}\,(p, s|x_0)}{\mathrm{d}x_0^2} - p\theta\,(x_0)\,\tilde{Q}\,(p, s|x_0) \tag{24}$$

which has to be solved according to the boundary conditions

$$\tilde{Q}\,(p, s|x_0 \to +\infty) = \frac{1}{s + p}, \quad \tilde{Q}\,(p, s|x_0 \to -\infty) = \frac{1}{s}. \tag{25}$$

To this end we need to specify the expression of $D(x)$. Once $\tilde{Q}(p, s|x_0)$ is known, one can find the PDF of $y = T^+/t$ in the long time limit by using the method in reference [41].

J. Stat. Mech. (2026) 013203

4.1. Piecewise heterogeneity

For the piecewise diffusion coefficient (12) we solve (24) in the regions $x_0 < 0$ and $x_0 > 0$ separately taking into account (25). We find

$$\begin{aligned}\tilde{Q}_-(p,s|x_0) &= \frac{1}{s} + A_1 \mathrm{e}^{x_0\sqrt{\frac{s}{D_-}}},\ x_0 < 0\\ \tilde{Q}_+(p,s|x_0) &= \frac{1}{s+p} + B_2 \mathrm{e}^{-x_0\sqrt{\frac{s+p}{D_+}}},\ x_0 > 0.\end{aligned} \tag{26}$$

The constants A_1 and B_2 can be found by requiring continuity of $\tilde{Q}$ and its derivative $\partial_{x_0}\tilde{Q}$ across $x_0 = 0$. This implies

$$\begin{aligned}\tilde{Q}_-(p,s|x_0 \to 0) &= \tilde{Q}_+(p,s|x_0 \to 0)\\ \left[\frac{\partial \tilde{Q}_-(p,s|x_0)}{\partial x_0}\right]_{x_0=0} &= \left[\frac{\partial \tilde{Q}_+(p,s|x_0)}{\partial x_0}\right]_{x_0=0}.\end{aligned} \tag{27}$$

Then introducing (26) into (27) and solving the resulting system of equations we obtain A_1 and B_2 and setting $x_0 = 0$ for simplicity into (26) we finally get

$$\tilde{Q}(p,s|0) = \frac{1}{s+p}\left(1 + \frac{p}{s+\gamma\sqrt{s(s+p)}}\right) \tag{28}$$

where

$$\gamma = \sqrt{\frac{D_-}{D_+}}$$

can be regarded as the asymmetry parameter. To invert the characteristic function (28) back to T^+ and t we note that it has the following scaling behavior

$$\tilde{Q}(p,s|0) = \frac{1}{s} g\left(\frac{p}{s}\right).$$

Then the random variable $y = T^+/t$ possesses the distribution

$$P(y|0) = P\left(y = \frac{T^+}{t}, t|0\right) = tP\left(T^+ = yt, t|0\right)$$

which can be computed as was done in [41] by noting

$$P(y|0) = -\frac{1}{\pi y}\lim_{\epsilon\to 0}\mathrm{Im}\left[g\left(-\frac{1}{y+i\epsilon}\right)\right]. \tag{29}$$

J. Stat. Mech. (2026) 013203

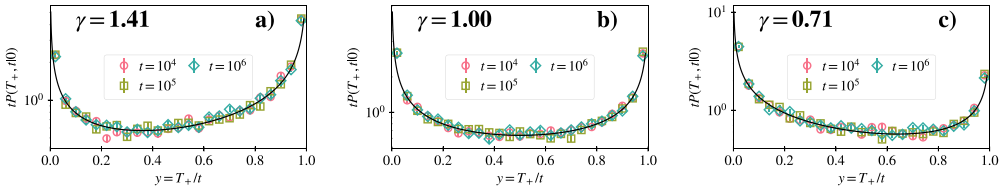

Figure 1. Limiting distribution of the half-occupation time for the piecewise heterogeneity. The different symbols are for trajectories with $t = 10^4, 10^5$, and 10^6. The black solid line corresponds to equation (31). $D_+ = 0.5, 1.0$, and 2.0 in panels (a), (b), and (c), respectively. In all panels $D_- = 1.0$, $x_0 = 0$, simulation timestep $\mathrm{d}t = 0.1$, and $N = 10^4$ trajectories.

Thus, from (28)

$$g(\chi) = \frac{1}{1+\chi}\left(1 + \frac{\chi}{1+\gamma\sqrt{1+\chi}}\right)$$

where $\chi = p/s$. Setting $\chi^{-1} = -y - i\epsilon$ and computing (29) we find the *asymmetric arcsine* PDF

$$P\left(T^+, t|0\right) = \frac{1}{t}F\left(\frac{T^+}{t}\right) \tag{30}$$

where

$$F(y) = \frac{\gamma}{\pi\sqrt{y(1-y)}\left[y + \gamma^2(1-y)\right]}.$$

Thus, from (29),

$$P(y|0) = \frac{\gamma}{\pi\sqrt{y(1-y)}\left[y + \gamma^2(1-y)\right]}, \quad 0 < y < 1. \tag{31}$$

The same limiting distribution has been obtained for a random walk in one dimension under an asymmetric force field acting on a finite region [42]. Although there is no a general direct correspondence, in a way, the confining effect of the asymmetric force field is physically analogous to a heterogeneous media with constant asymmetric diffusion coefficient. In figure 1 we test the result (31) against numerical simulations. We see that for sufficiently large values of t, $tP(T^+, t|0)$ converges to the limiting distribution $F(y)$. Unlike for the arcsine case, the minimum of $F(y)$ is not located at $y = 1/2$ as can be also observed in figure 1. It is located at

$$y_{\min} = \frac{5\gamma^2 - 3 - \sqrt{9\gamma^4 - 14\gamma^2 + 9}}{8(\gamma^2 - 1)}.$$

From this expression and also from figure 1 we see that if $\gamma > 1$ then $y_{\min}$ moves to the left while if $\gamma < 1$ it moves to the right. For $\gamma = 1$, $y_{\min} = 1/2$ as expected.

J. Stat. Mech. (2026) 013203

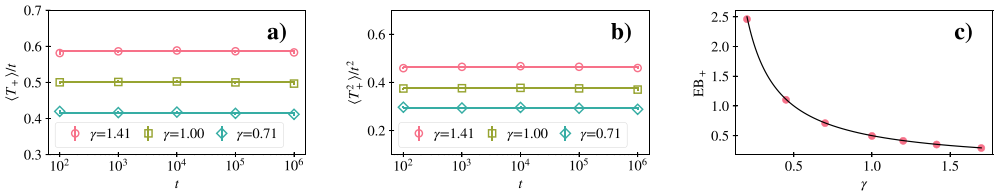

Figure 2. (a) $\langle T^+(t)\rangle$, (b) $\langle T^+(t)^2\rangle$, and (c) EB_+ of the half-occupation time for the piecewise heterogeneity. In panels (a), and (b) the solid lines are computed with equation (32), $D_+ = 0.5, 1.0$, and 2.0; In panel (c) the solid line is equation (33). In all panels $D_- = 1.0$, $x_0 = 0$, simulation timestep $\mathrm{d}t = 0.1$, and $N = 10^4$ trajectories.

The two first moments of $P(T^+, t|0)$ can be found from (6) with (28) or from (31). In any case we find

$$\left\langle T^+(t)\right\rangle = \frac{\gamma}{\gamma+1}t, \quad \left\langle T^+(t)^2\right\rangle = \frac{\gamma(1+2\gamma)}{2(\gamma+1)^2}t^2. \tag{32}$$

Note first that $\langle T^+(t)\rangle > t/2$ (the time spent at $x>0$ is in average higher than half of the total time) if $\gamma > 1$, this is, if $D_- > D_+$. This is expected since in this case the motion of the particle is slower in the region $x>0$ than in the region $x<0$. Note also that the coefficient $\gamma/(1+\gamma)$ in (32) corresponds to the probability that the particle is at $x>0$.

If $D_- = D_+$ one has $\gamma = 1$ and the two moments (32) reduce to the values corresponding to the BM in a homogeneous media. In addition, when $\gamma = 1$ equation (31) turns into the *arcsine law* [43]. Now, we are in position to compute the ergodicity breaking parameter. From (19) and (32) we finally find

$$\mathrm{EB}_+ = \frac{\left\langle T^+(t)^2\right\rangle}{\left\langle T^+(t)\right\rangle^2} - 1 = \frac{1}{2\gamma}, \tag{33}$$

which predicts a non-ergodic behavior regardless of the values of γ.

In figure 2 we compare (32) and (33) with numerical simulations. The greater D_- is in comparison to D_+, the greater γ is, therefore the probability that the particle is at $x>0$ increases, and thus the time spent there also is greater. This is captured by EB_+ which decreases with γ as expected.

Finally, we compute the PDF of the time average of the observable $\theta[x(t)]$, this is, the PDF of the time averaged occupation fraction

$$\eta_+ = \lim_{t\to\infty} \frac{T^+}{\langle T^+(t)\rangle} \tag{34}$$

J. Stat. Mech. (2026) 013203

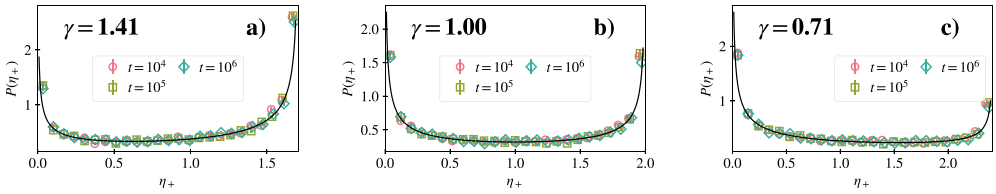

Figure 3. PDF of the time averaged half-occupation time for the piecewise heterogeneity. The different symbols are for trajectories with $t = 10^4, 10^5$, and 10^6. $D_+ = 0.5, 1.0$, and 2.0 in panels (a), (b), and (c), respectively. The solid line is computed with equation (35) In all panels $D_- = 1.0$, $x_0 = 0$, simulation timestep $\mathrm{d}t = 0.1$, and $N = 10^4$ trajectories.

as defined in equation (21). It can be obtained from the limiting distribution $P(y|0)$ by simply accounting for the relation between the variables y and η_+. We find from (31) the density

$$\begin{aligned} P(\eta_+) &= \frac{\gamma}{\gamma+1} P\left(y = \frac{\gamma}{\gamma+1}\eta_+\right) \\ &= \frac{\gamma}{\pi(\gamma+\eta_+-\gamma\eta_+)\sqrt{\gamma\eta_+(1+\gamma-\gamma\eta_+)}} \end{aligned} \tag{35}$$

where $0 < \eta_+ < (\gamma+1)/\gamma$. In figure 3 we compare equation (35) with numeric simulations.

4.2. Power law heterogeneity

For the power law diffusion coefficient (9) we solve (24) in the regions $x_0 < 0$ and $x_0 > 0$ separately. The solution for the characteristic function is

$$\tilde{Q}(p, s|0) = \frac{1}{s+p}\left[1 + \frac{p/s}{1+\left(\frac{s+p}{s}\right)^{\frac{1}{2-\alpha}}}\right], \quad \alpha < 1 \tag{36}$$

for $x_0 = 0$ (see appendix A for details of the derivation).

To invert (36) to the real space, one can follow the same method employed for the piecewise heterogeneity. Thus, from (29)

$$g(\chi) = \frac{1}{1+\chi}\left[1 + \frac{\chi}{1+(1+\chi)^{\frac{1}{2-\alpha}}}\right],$$

so that

$$P(T^+, t|0) = \frac{1}{t} G_{\frac{2}{2-\alpha}}\left(\frac{T^+}{t}\right) \tag{37}$$

J. Stat. Mech. (2026) 013203

where the scaling function is

$$G_{\frac{2}{2-\alpha}}(y)=\frac{\sin\left(\frac{\pi}{2-\alpha}\right)}{\pi}\frac{\left[y(1-y)\right]^{\frac{-1+\alpha}{2-\alpha}}}{y^{\frac{2}{2-\alpha}}+(1-y)^{\frac{2}{2-\alpha}}+2\cos\left(\frac{\pi}{2-\alpha}\right)\left[y(1-y)\right]^{\frac{1}{2-\alpha}}}.$$

for $\alpha<1$ with $y=T^{+}/t$. Thus, the PDF for y reads

$$P(y|0)=\frac{\sin\left(\frac{\pi}{2-\alpha}\right)}{\pi}\frac{\left[y(1-y)\right]^{\frac{-1+\alpha}{2-\alpha}}}{y^{\frac{2}{2-\alpha}}+(1-y)^{\frac{2}{2-\alpha}}+2\cos\left(\frac{\pi}{2-\alpha}\right)\left[y(1-y)\right]^{\frac{1}{2-\alpha}}} \tag{38}$$

for $0<y<1$. This result has been found in [35] by other means, but it is included here for completeness. However, the ergodic properties discussed below have not been explored in [35]. Equation (37) is the Lamperti PDF with index $2/(2-\alpha)$ which has been obtained in [44, 45] for a particle moving subdiffusively. However, equation (38) holds both when the underlying random walk is subdiffusive ($\alpha<0$) or superdiffusive ($0<\alpha<1$). Note also that in the limit $\alpha\to 0$ (homogeneous case) equation (38) reduces to the arcsine law as expected. Moreover, it can be shown that equation (38) possess a local maximum at $y=1/2$ when the heterogeneity is strong enough, this is, when the exponent α is high enough. The heterogeneity introduced through the spatial dependence given in equation (9) induces the particle to move in a region close to the origin, where the diffusion coefficient attains its minimum value. As α increases this region shrinks. This effect prevents the particle from performing excursions of long duration and forces the particle to revisit the origin more frequently. Thus, if $\alpha>\alpha_c$ a maximum of $P(y|0)$ appears at $y=1/2$ ($T^{+}=t/2$). When $\alpha<\alpha_c$ this peak disappears and $P(y|0)$ attains a U shape, indicating that the particle spends almost its entire time in one side ($x<0$ or $x>0$) only. To find α_c we impose the condition $(\mathrm{d}P(y|0)/\mathrm{d}y)_{y=1/2}=0$ for the PDF given in equation (38). Thus, α_c is the solution to the nonlinear equation

$$\cos\left(\frac{\pi}{2-\alpha_c}\right)=\frac{4\alpha_c-2-\alpha_c^2}{(2-\alpha_c)^2}$$

whose numerical solution is $\alpha_c\simeq 0.318$. It is easy to show that $P(y|0)\sim y^{-\frac{1-\alpha}{2-\alpha}}$ and

$$P(y|0)\sim(1-y)^{-\frac{1-\alpha}{2-\alpha}}$$

when y is close to 0 and 1, respectively. Then, $P(y|0)$ diverges at $y=0$ and at $y=1$. In consequence, (38) has two possible shapes, a U shape if $\alpha<0.318$ or a W shape if $\alpha>0.318$; both cases are shown in figure 4(panels (a) and (b)). In panel (c) we compare the limiting distribution obtained from simulations for $\alpha=1.5$ with (43) in the Laplace space, this is, with $P(u|0)=\mathcal{L}_{y\to u}[P(y|0)]=\mathcal{L}_{y\to u}[\delta(y-1)]=\mathrm{e}^{-0.5u}$. In the inset we show the plot in the real space. In all panels we plot data for different t to illustrate the convergence to the limiting distribution.

Transitions in the shape of the limiting distribution of T_{+}/t have been discussed across systems with distinct confining mechanisms, such as in diffusion and subdiffusion with power-law stochastic resetting [46], or for CTRW in a box [47]. In these cases,

J. Stat. Mech. (2026) 013203

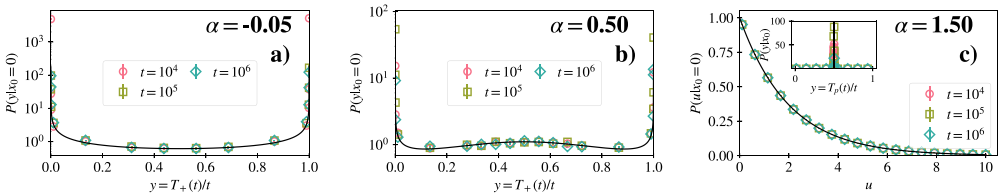

Figure 4. Limiting distribution of the half-occupation time for the power-law heterogeneity. The different symbols are for trajectories with $t = 10^4, 10^5$, and 10^6. In panels (a), and (b) the black solid line corresponds to equation (38); In panel (c) corresponds to $\mathrm{e}^{-0.5u}$, and to $\delta(t-0.5)$ in its inset. $\alpha = -0.05, 0.5$, and 1.5 in panels (a), (b), and (c), respectively. If $\alpha > 0$ $\epsilon = 10^{-10}$, and $\epsilon = 10^{-3}$ if $\alpha < 0$. In all panels $D_0 = 1.0$, $x_0 = 0$, simulation timestep $\mathrm{d}t = 0.1$, and $N = 10^4$ trajectories.

similarly to the one being discussed in the present work, the system gets progressively confined, and large excursions are hindered in favor of the system being more localized near the origin, giving rise to the change from a minimum to a maximum at $T_+/t = 1/2$. Moreover, in [48] a transition in the limiting PDF of T_+/t is discussed in terms of the number of walkers, and in [49] they discuss a change of shape in the PDF of T_+/t for Brownian motion with Poissonian resetting, during the transient behavior, converging to a delta function in the long time limit. All these studies highlight non-trivial behavior of the half occupation time.

Regarding the moments, the mean half occupation time and the mean squared half occupation time can be obtained from (36) and (6) as

$$\left\langle T^+(t)\right\rangle = \frac{t}{2}, \quad \left\langle T^+(t)^2\right\rangle = \frac{3-2\alpha}{4(2-\alpha)}t^2. \tag{39}$$

The ergodicity breaking parameter can be straightforwardly found from (19) and (39) as

$$\mathrm{EB}_+ = \frac{1-\alpha}{2-\alpha}, \quad \alpha \leqslant 1. \tag{40}$$

When $\alpha \to 1^-$ the expression for the characteristic function given by equation (36) reads

$$\tilde{Q}(p,s|0) = \frac{2}{2s+p} \tag{41}$$

which after the double Laplace inversion reads

$$P\left(T^+,t|0\right) = \delta\left(T^+ - \frac{t}{2}\right). \tag{42}$$

In this case the PDF for y reads

$$P(y|0) = \delta(y-1). \tag{43}$$

J. Stat. Mech. (2026) 013203

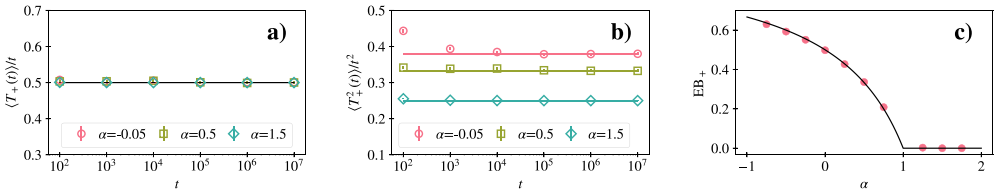

Figure 5. (a) $\langle T^+(t)\rangle$, (b) $\langle T^+(t)^2\rangle$, and (c) EB_+ of the half-occupation time for the power-law heterogeneity. In panels (a), and (b) the solid lines are computed with equation (39) and $\alpha = -0.05, 0.5$, and 1.5; In panel (c) the solid line is equation (40). If $\alpha > 0$ $\epsilon = 10^{-10}$, and $\epsilon = 10^{-3}$ if $\alpha < 0$. In all panels $D_0 = 1.0$, $x_0 = 0$, simulation timestep $\mathrm{d}t = 0.1$, and $N = 10^4$ trajectories.

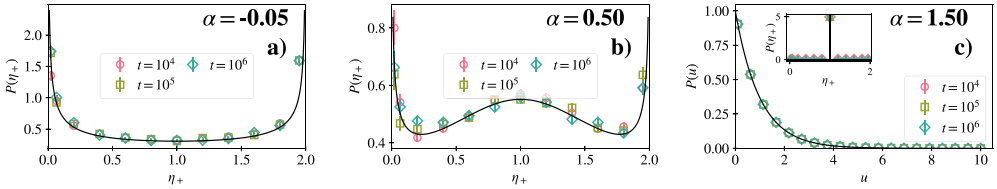

Figure 6. PDF of the time averaged half-occupation time for the power-law heterogeneity. The different symbols are for trajectories with $t = 10^4, 10^5$, and 10^6. The black solid line corresponds to equation (44) in panels (a), and (b); to e^{-u} in panel (c), and to $\delta(t-1)$ in its inset. $\alpha = -0.05, 0.5$, and 1.5 in panels (a), (b), and (c), respectively. If $\alpha > 0$ we take $\epsilon = 10^{-10}$, and $\epsilon = 10^{-3}$ if $\alpha < 0$. In all panels $D_0 = 1.0$, $x_0 = 0$, simulation timestep $\mathrm{d}t = 0.1$, and $N = 10^4$ trajectories.

This means that when $\alpha \to 1^-$, the half occupation time is always $t/2$, coinciding with its mean value. Likewise, it can also be seen that, in this case, $\mathrm{EB}_+ = 0$, i.e. the process is ergodic. Therefore, there is an ergodic transition at $\alpha = 1$. This transition can be understood by the effect of the heterogeneity, which, for $\alpha \geqslant 1$ is strong enough to localize the particles near the origin, preventing large excursions. Interestingly, the transition to the ergodic phase occurs across the value of α corresponding to the ballistic regime, $\alpha = 1$. To ensure an ergodic behavior the transport regime has to be super-ballistic in order to avoid the confining effect of the heterogeneity. Figure 5 compares (39) and (40) with numerical simulations. It can be noticed the ergodic transition at $\alpha = 1$ in panel 5(c).

The PDF for the time averaged observable $\theta[x(t)]$ (this is η_+ defined in (34)) can be obtained from (38) noting that $\eta_+ = 2y$ to get

$$P(\eta_+) = \frac{\sin\left(\frac{\pi}{2-\alpha}\right)}{\pi} \frac{2\left[\eta_+(2-\eta_+)\right]^{\frac{-1+\alpha}{2-\alpha}}}{\eta_+^{\frac{2}{2-\alpha}} + (2-\eta_+)^{\frac{2}{2-\alpha}} + 2\cos\left(\frac{\pi}{2-\alpha}\right)\left[\eta_+(2-\eta_+)\right]^{\frac{1}{2-\alpha}}} \tag{44}$$

for $0 < \eta_+ < 2$. In figure 6 we compare equation (44) to numerical simulations.

J. Stat. Mech. (2026) 013203

5. Occupation time in an interval

We consider now the occupation time $T_a(t|x_0)$ of the random particle in an interval $[-a,a]$ up to time t if starting initially from x_0. In this case, the function $U(x_0)=\theta(-a<x_0<a)$. The corresponding Feynman–Kac equation (8) needs to be solved with suitable boundary conditions. For instance, if the starting point is at infinity i.e. $x_0\to\pm\infty$ the particle will never reach the interval so that $P(T_a,t|x_0\to\pm\infty)=\delta(T_a)$, i.e. $\tilde{Q}(p,s|x_0\to\pm\infty)=1/s$. The initial condition is such that $T_a(t=0|x_0)=0$ so that $Q(p,t=0|x_0)=1$. Thus, the Feynman–Kac equation for $\tilde{Q}(p,s|x_0)$ to be solve in the Laplace space is

$$s\tilde{Q}\left(p,s|x_0\right)-1=D\left(x_0\right)\frac{\mathrm{d}\tilde{Q}\left(p,s|x_0\right)}{\mathrm{d}x_0^2}-p\theta\left(-a<x_0<a\right)\tilde{Q}\left(p,s|x_0\right) \tag{45}$$

under the above boundary conditions. It must be explicitly found in the regions I ($x_0<-a$), II ($-a<x_0<0$), III ($0<x_0<a$) and IV ($x_0>a$).

5.1. Piecewise heterogeneity

The solution of equation (45) for the piecewise diffusion coefficient (12) is given by (setting $x_0=0$)

$$\tilde{Q}\left(p,s|0\right)=\frac{1}{s+p}\left[1+\frac{p}{sF\left(s,p\right)}\right] \tag{46}$$

where

$$F\left(s,p\right)=\frac{M_-\left(s,p\right)N_+\left(s,p\right)+\gamma M_+\left(s,p\right)N_-\left(s,p\right)}{N_+\left(s,p\right)+\gamma N_-\left(s,p\right)}$$

and

$$\begin{aligned}M_\pm\left(s,p\right)&=\cosh\left(a\sqrt{\frac{s+p}{D_\pm}}\right)+\sqrt{\frac{s+p}{s}}\sinh\left(a\sqrt{\frac{s+p}{D_\pm}}\right)\\ N_\pm\left(s,p\right)&=\sinh\left(a\sqrt{\frac{s+p}{D_\pm}}\right)+\sqrt{\frac{s+p}{s}}\cosh\left(a\sqrt{\frac{s+p}{D_\pm}}\right).\end{aligned}$$

Since the double Laplace inversion of $\tilde{Q}(p,s|0)$ cannot be found explicitly we derive an approximate expression which holds when t and T_a are large. To do this, we consider s and p small and comparable in equation (46) and find

$$\tilde{Q}\left(p,s|0\right)\simeq\frac{1}{s+p}\left[1+\frac{p}{s+\mathcal{C}\sqrt{s}\left(s+p\right)}\right] \tag{47}$$

J. Stat. Mech. (2026) 013203

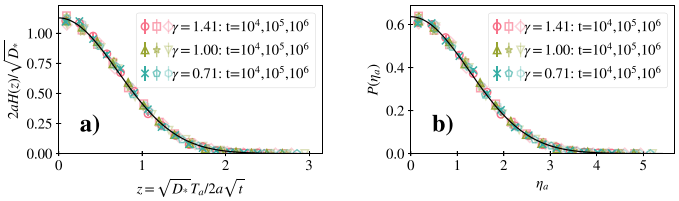

Figure 7. (a) Limiting distribution of the occupation time in the interval $[-3,3]$ for the piecewise heterogeneity. The black solid line corresponds to equation (48). (b) PDF of the time averaged occupation time in the interval $[-3,3]$ for the piecewise heterogeneity. The black solid line corresponds to equation (52). In all panels, the symbols of the same color are for $D_+ = 0.5, 1.0$, and 2.0 salmon, green, and blue, respectively. The different symbol shapes are for trajectories with $t = 10^4, 10^5$, and 10^6. $D_- = 1.0$, $x_0 = 0$, simulation timestep $\mathrm{d}t = 0.1$, and $N = 10^4$ trajectories.

where

$$\mathcal{C} = \frac{a}{\sqrt{D_+} + \sqrt{D_-}} \left(\sqrt{\frac{D_+}{D_-}} + \sqrt{\frac{D_-}{D_+}} \right).$$

Performing the double Laplace inversion of (47), we find that the PDF of T_a obeys the half-Gaussian density

$$P\left(T_a, t|0\right) \sim \frac{1}{t^{1/2}} H\left(\frac{\sqrt{D_*}T_a}{2a\sqrt{t}}\right) \tag{48}$$

where the scaling function is

$$H\left(z\right) = \sqrt{\frac{D_*}{a^2\pi}} \mathrm{e}^{-z^2}, \quad D_* = \left(\frac{D_+\sqrt{D_-} + D_-\sqrt{D_+}}{D_+ + D_-} \right)^2.$$

In panel (a) of figure 7 we check (48) against numerical solutions for different values of γ. We also add data computed for different large values of t to show that when t is sufficiently large the numerical results fall on the theoretical curve.

The mean and mean square occupation time can be computed from (46) and (6) as

$$\left\langle T_a\left(t\right)\right\rangle \simeq \frac{2a\sqrt{t}}{\sqrt{\pi}\, D_*}, \quad \left\langle T_a\left(t\right)^2\right\rangle \simeq \frac{2a^2}{D_*} t. \tag{49}$$

It is interesting to note that in the long time limit the PDF $P(T_a, t|0)$ can be corresponds to the PDF for the Brownian motion moving in a homogeneous media [50] with an effective diffusion coefficient D_*. The ergodicity breaking parameter can be found

J. Stat. Mech. (2026) 013203

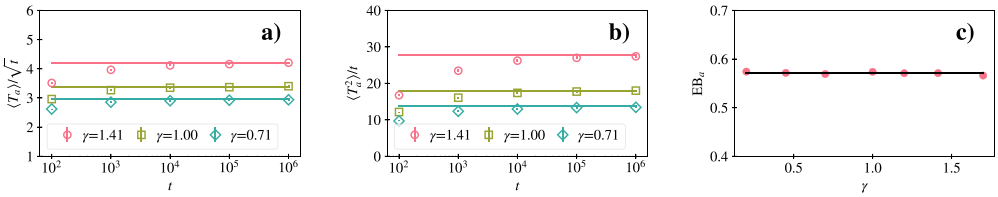

Figure 8. (a) $\langle T_a(t)\rangle$, (b) $\langle T_a(t)^2\rangle$, and (c) EB_a of the half-occupation time for the piecewise heterogeneity. In panels (a), and (b) the solid lines are computed with equation (49), $D_+ = 0.5, 1.0$, and 2.0; In panel (c) the solid line is equation (50). In all panels $D_- = 1.0$, $x_0 = 0$, simulation timestep $\mathrm{d}t = 0.1$, and $N = 10^4$ trajectories. In panels (a), and (b) the interval is $[-3, 3]$ and in panel (c) the interval is $[-0.5, 0.5]$.

from (19) and (49) to get

$$\mathrm{EB}_a = \frac{\left\langle T_a(t)^2 \right\rangle}{\langle T_a(t)\rangle^2} - 1 = \frac{\pi}{2} - 1 \tag{50}$$

which is the same as the EB parameter for the Brownian motion in homogeneous media. This means that in the long time limit the ergodic properties in terms of the occupation time in an interval for a Brownian particle are not altered by the piecewise heterogeneity. In figure 8 we compare (49) and (50) with numerical simulations.

In the short-time limit, when both s and p are large and comparable we find that the leading term in the asymptotic expansion in equation (46) is $\tilde{Q}(p, s|0) \sim 1/(s+p)$ which turns into $P(T_a, t|0) \sim \delta(T_a - t)$. This is consistent with the fact that for short times the particle will have barely moved and will have spent most of its time within the interval.

Now we find the PDF of the time average of the observable $\theta[-a < x(t) < a]$ in the long time limit, this is, the PDF of

$$\eta_a = \lim_{t\to\infty} \frac{T_a}{\langle T_a(t)\rangle}, \tag{51}$$

as defined in equation (21). For the piecewise diffusion coefficient

$$\eta_a = \frac{T_a}{2a}\sqrt{\frac{\pi D_*}{t}}$$

and its PDF follows from (22) and (48). In this case we readily find

$$P(\eta_a) = \mathcal{M}_{1/2}(\eta_a) = \frac{2}{\pi} \mathrm{e}^{-\frac{\eta_a^2}{\pi}}, \tag{52}$$

which is the same result as for BM in a homogeneous media. In panel b) of figure 7 we compare (52) with numerical simulations. We note that the PDF $P(\eta_a)$ computed for different values of the asymmetry parameter γ collapse on the same curve, which

J. Stat. Mech. (2026) 013203

confirms that $P(\eta_a)$ does not depend on γ. In addition, it can be observed how the distribution converges to the theoretical result (52) in the long time limit.

5.2. Power law heterogeneity

In this case the expression for the characteristic function in the long time limit is given by (see details of the derivation in appendix C)

$$\tilde{Q}(p,s|0) \simeq \frac{\lambda_\alpha + s^{-1+\frac{1}{2-\alpha}}}{s^{\frac{1}{2-\alpha}} + \lambda_\alpha (s+p)} \tag{53}$$

which holds for $\alpha < 1$ and where we have defined

$$\lambda_\alpha = \frac{a^{1-\alpha}}{\left[(2-\alpha)\sqrt{D_0}\right]^{\frac{2-2\alpha}{2-\alpha}}} \frac{\Gamma\left(\frac{1}{2-\alpha}\right)}{\Gamma\left(\frac{3-2\alpha}{2-\alpha}\right)}.$$

Before proceeding to invert in Laplace this result we note that for $\alpha < 1$ we can further simplify this expression by noting that in the limit $s \to 0$ we have $s \ll s^{\frac{1}{2-\alpha}}$ and thus

$$\tilde{Q}(p,s|0) \simeq \frac{s^{-1+\frac{1}{2-\alpha}}}{s^{\frac{1}{2-\alpha}} + \lambda_\alpha p}. \tag{54}$$

Performing the Laplace inversion of (54) with respect to p one readily finds

$$Q(T_a,s|0) \simeq \frac{s^{-1+\frac{1}{2-\alpha}}}{\lambda_\alpha} \exp\left(-s^{\frac{1}{2-\alpha}} \frac{T_a}{\lambda_\alpha}\right) \tag{55}$$

We next compute the Laplace inversion of (55) with respect to s using

$$\mathcal{L}_s^{-1}\left(s^{\beta-1}\mathrm{e}^{-us^\beta}\right) = \frac{t}{\beta u^{1+1/\beta}} l_\beta\left(\frac{t}{u^{1/\beta}}\right)$$

where $l_\beta(\cdot)$ is the one-sided Lévy density with order β. We thus find the scaling form

$$P(T_a,t|0) \sim \frac{1}{t^{\frac{1}{2-\alpha}}} N_\alpha\left(\frac{T_a}{\lambda_\alpha t^{\frac{1}{2-\alpha}}}\right) \tag{56}$$

for $\alpha < 1$, where the scaling function $N_\alpha(z)$ reads

$$N_\alpha(z) = \frac{2-\alpha}{\lambda_\alpha z^{3-\alpha}} l_{\frac{1}{2-\alpha}}\left(\frac{1}{z^{2-\alpha}}\right).$$

In the limit $\alpha \to 1^-$ we see that (54) turns into

$$\tilde{Q}(p,s|0) \simeq \frac{1}{s+p} \tag{57}$$

J. Stat. Mech. (2026) 013203

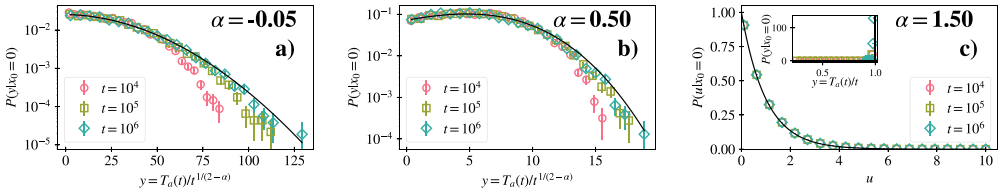

Figure 9. Limiting distribution of the occupation time in the interval $[-20,20]$ for the power-law heterogeneity. The different symbols are for trajectories with $t=10^4,10^5$, and 10^6. The black solid line corresponds to equation (56) in panels (a), and (b); to e^{-u} in panel (c), and to equation (58) in its inset. $\alpha=-0.05,0.5$, and 1.5 in panels (a), (b), and (c), respectively. If $\alpha>0$ $\epsilon=10^{-10}$, and $\epsilon=10^{-3}$ if $\alpha<0$. In all panels $D_0=1.0$, $x_0=0$, simulation timestep $\mathrm{d}t=0.1$, and $N=10^4$ trajectories.

which after Laplace inversion yields

$$P\left(T_a,t|0\right)\simeq\delta\left(T_a-t\right),\quad \alpha\to1^{-}. \tag{58}$$

It is worth observing that at $\alpha=1$ there is a transition in the behavior of the PDF $P(T_a,t|0)$. For $1\leqslant\alpha<2$ the heterogeneity is so strong that the particle cannot escape the interval $[-a,a]$ for any a, which is reflected in the fact that T_a is equal to t.

The comparison of the limiting distributions given in equations (56) and (58) with numerical simulations is shown in figure 9. We note that the PDFs converge to the theoretical results in the long time limit in panels a) and b). In panel c) we show the limiting distribution for a value of $\alpha>1$ in the Laplace space. In this case the observable is ergodic, i.e. the limiting distribution is given by (58). The inset shows the limiting distribution in the real space.

On the other hand, using (54) we can compute the two first moments. The mean and mean square occupation time are

$$\left\langle T_a\left(t\right)\right\rangle\simeq\frac{\lambda_\alpha}{\Gamma\left(\frac{3-\alpha}{2-\alpha}\right)}t^{\frac{1}{2-\alpha}},\quad \left\langle T_a\left(t\right)^2\right\rangle\simeq\frac{2\lambda_\alpha^2}{\Gamma\left(\frac{4-\alpha}{2-\alpha}\right)}t^{\frac{2}{2-\alpha}}. \tag{59}$$

Likewise, the ergodicity breaking parameter can be found from (19) and (59) to get

$$\mathrm{EB}_a=\frac{\left\langle T_a\left(t\right)^2\right\rangle}{\left\langle T_a\left(t\right)\right\rangle^2}-1=\begin{cases}\frac{2\Gamma\left(\frac{3-\alpha}{2-\alpha}\right)^2}{\Gamma\left(\frac{4-\alpha}{2-\alpha}\right)}-1, & \alpha<1\\ 0, & 1<\alpha<2.\end{cases} \tag{60}$$

Note that at $\alpha=1$ there is an ergodic transition between non-ergodic phase $\alpha<1$ and ergodic phases $\alpha>1$, like for the half occupation time. The results given in (56) and (60) have been previously obtained in reference [19] by assuming that the PDF of T_a can be given by the PDF of the number of returns to the interval $[-a,a]$. This assumption

J. Stat. Mech. (2026) 013203

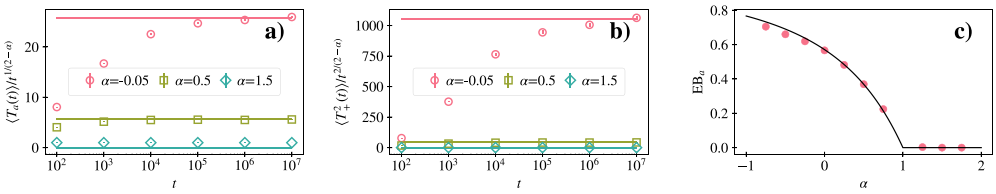

Figure 10. (a) $\langle T_a(t)\rangle$, (b) $\langle T_a(t)^2\rangle$, and (c) EB_a of the occupation time in the interval [-20,20] for the power-law heterogeneity. In panels (a), and (b) the solid lines are computed with equation (59) and $\alpha=-0.05, 0.5$, and 1.5; in panel (c) the solid line is equation (60). We take $\alpha>0$ if $\epsilon=10^{-10}$, and $\epsilon=10^{-3}$ if $\alpha<0$. In all panels $D_0=1.0$, $x_0=0$, simulation timestep $\mathrm{d}t=0.1$, and $N=10^4$ trajectories.

requires that the returns constitute a renewal process [42], i.e. the times between successive returns are uncorrelated, which is not true for any general process. However, we have obtained the same results without making any further assumption, but by directly solving the corresponding Feynman–Kac equation.

In figure 10 we compare the theoretical results for the two first moments given in equations (59) and (60) with numerical simulations. It is worth mentioning that for $\alpha<0$ the convergence to the analytic result is slower the smaller α is. Note also that EB_a and EB_+ vs α in panels 5(c) and 10(c) look qualitatively very similar and be regarded as phase diagrams of the ergodic properties.

In the short-time limit we consider the asymptotic expansion of equations (C5) and (C6) for large s and p. As for the piecewise heterogeneity, in this limit the PDF for the occupation time in an interval is $P(T_a,t|0)\sim\delta(T_a-t)$. Again, showing that at short times the particle will not have escaped the interval.

Next, we compute the PDF for the time average of the observable $\theta[-a<x(t)<a]$ in the long time limit. From (51) and (49)

$$\eta_a=\frac{T_a}{\lambda_\alpha t^{\frac{1}{2-\alpha}}}\Gamma\left(\frac{3-\alpha}{2-\alpha}\right)$$

and from (56), we find that in the long time limit $P(\eta_a)$ is given by the Mittag–Leffler (ML) distribution of order β:

$$P(\eta_a)=\mathcal{M}_\beta(\eta_a)=\frac{\Gamma(1+\beta)^{\frac{1}{\beta}}}{\beta\eta_a^{1+\frac{1}{\beta}}}l_\beta\left[\frac{\Gamma(1+\beta)^{\frac{1}{\beta}}}{\eta_a^{\frac{1}{\beta}}}\right],\quad \beta=\frac{1}{2-\alpha} \tag{61}$$

for $\alpha<1$. The PDF given in (61) depends on neither D_0 nor a but only on α. This result is checked with numerical simulations as shown in figure 11. For $\alpha>1$ the PDF of time averaged occupation time in the interval is $P(\eta_a)=\delta(\eta_a-1)$, according to (58). In panels (a) and (b) we show two cases for $\alpha<1$ while in panel c) we show a case for $\alpha>1$ in the Laplace space. In the inset of panel (c) we show the same PDF but in the real space.

J. Stat. Mech. (2026) 013203

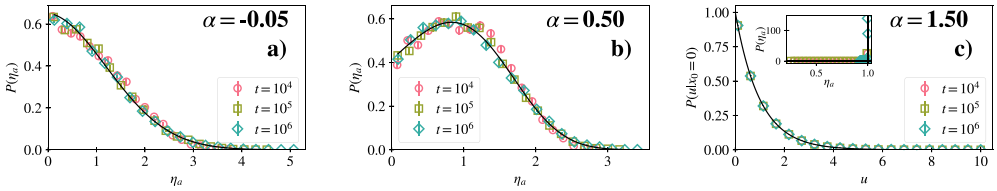

Figure 11. PDF of the time averaged occupation time in the interval $[-20,20]$ for the power-law heterogeneity. The different symbols are for trajectories with $t=10^4,10^5$, and 10^6. The black solid line corresponds to equation (61) in panels (a), and (b); to e^{-u} in panel (c), and to $\delta(\eta_a-1)$ in its inset. $\alpha=-0.05,0.5$, and 1.5 in panels (a), (b), and (c), respectively. If $\alpha>0$ $\epsilon=10^{-10}$, and $\epsilon=10^{-3}$ if $\alpha<0$. In all panels $D_0=1.0$, $x_0=0$, simulation timestep $\mathrm{d}t=0.1$, and $N=10^4$ trajectories.

6. Conclusions

In this work, we analyzed the ergodic properties of Brownian motion in heterogeneous media through the statistics of the occupation time. By solving the Feynman–Kac equation associated with the characteristic function of the occupation times, we obtained analytical results for two relevant forms of spatially varying diffusion coefficient: a piecewise-constant model and a power-law dependence. From these solutions, we derived the limiting distributions of the occupation times, their first two moments, and the corresponding EB parameters, finding excellent agreement with numerical simulations.

For the piecewise diffusion coefficient, we showed that the probability density of the half occupation time follows an asymmetric arcsine law, with a strictly positive EB parameter. The distribution of the occupation time within an interval is half-Gaussian-analogous to the homogeneous case but with an effective diffusion coefficient–and the EB parameter matches that of standard Brownian motion, confirming non-ergodic behavior in terms of both occupation times.

For the power-law diffusion coefficient, our results reproduce the occupation-time distributions previously obtained in references [19, 35], but reveal a transition between non-ergodic and ergodic phases. As the exponent α increases, the system evolves from a non-ergodic regime for $\alpha<1$ to an ergodic for $\alpha>1$. Unlike other models of anomalous diffusion in which the ergodic transition occurs when the MSD ranges from subdiffusive to normal regimes [47], when the anomalous diffusion is generated by a power-law spatially dependent diffusion coefficient, the ergodic transition takes place when the MSD ranges from superdiffusive to super-ballistic regimes in the Itô interpretation.

Overall, this study illustrates how the Feynman–Kac formalism provides a powerful framework to characterize ergodic properties of diffusion processes in heterogeneous media. While we focused on two specific spatial dependencies of the diffusion coefficient, the approach can be extended to more general forms [5]. The spatial dependence of the diffusion coefficient in the Langevin equation can be regarded as the random motion of a particle in heterogeneous temperature fields which can hinder or promote ergodicity.

J. Stat. Mech. (2026) 013203

Our results could be relevant to model heat conduction, where chains of oscillators with spatially varying local thermostats use position-dependent Langevin baths [51].

Acknowledgments

The authors acknowledge the financial support of the Ministerio de Ciencia e Innovación (Spanish government) under Grant No. PID2021-122893NB-C22.

Appendix A. Derivation of equation (36)

In the region I, $x_0 \in (-\infty, 0]$, the equation for the characteristic function is

$$D_0|x_0|^\alpha \frac{\mathrm{d}\tilde{Q}_I(p,s|x_0)}{\mathrm{d}x_0^2} - s\tilde{Q}_I(p,s|x_0) = -1$$

while in the region II, $x_0 \in [0, +\infty)$, one has

$$D_0|x_0|^\alpha \frac{\mathrm{d}\tilde{Q}_{II}(p,s|x_0)}{\mathrm{d}x_0^2} - (s+p)\,\tilde{Q}_{II}(p,s|x_0) = -1.$$

The above equations can be identified with a Lommel-type equation (see equation 8.491.11 in reference [52])

$$\frac{\mathrm{d}^2 u(z)}{\mathrm{d}z^2} - \omega^2\rho^2 z^{2\omega-2} u(z) = 0$$

which admits the solution

$$u(z) = \sqrt{z}\left[c_1 K_{\frac{1}{2\omega}}(\rho z^\omega) + c_2 I_{\frac{1}{2\omega}}(\rho z^\omega)\right],$$

where $K(\cdot)$ and $I(\cdot)$ are the modified Bessel functions. Identifying

$$\omega = \frac{2-\alpha}{2}, \quad \rho = \frac{2}{2-\alpha}\sqrt{\frac{s}{D_0}}$$

the solutions in regions I and II under the boundary conditions $\tilde{Q}(p,s|x_0 \to \pm\infty) < \infty$ are

$$\begin{aligned}
\tilde{Q}_I(p,s|x_0) &= \frac{1}{s} + A_1|x_0|^{1/2} K_{\frac{1}{2-\alpha}}\left(\frac{2}{2-\alpha}|x_0|^{1-\frac{\alpha}{2}}\sqrt{\frac{s}{D_0}}\right), \; x_0 < 0 \\
\tilde{Q}_{II}(p,s|x_0) &= \frac{1}{s+p} + A_2 x_0^{1/2} K_{\frac{1}{2-\alpha}}\left(\frac{2}{2-\alpha}x_0^{1-\frac{\alpha}{2}}\sqrt{\frac{s+p}{D_0}}\right), \; x_0 > 0.
\end{aligned} \tag{A1}$$

J. Stat. Mech. (2026) 013203

To compute the constants A_1 and A_2 we proceed to match both solutions and their derivatives at $x_0 = 0$:

$$\begin{aligned} \tilde{Q}_I(p,s|x_0 \to 0) &= \tilde{Q}_{II}(p,s|x_0 \to 0) \\ \left[\frac{\partial \tilde{Q}_I(p,s|x_0)}{\partial x_0}\right]_{x_0=0} &= \left[\frac{\partial \tilde{Q}_{II}(p,s|x_0)}{\partial x_0}\right]_{x_0=0} \end{aligned} \tag{A2}$$

Introducing (A1) into (A2) and making use of the approximation of the modified Bessel function for small argument

$$\lim_{x_0\to 0}\left[x_0^{\mu}K_{\nu}(cx_0^{\sigma})\right] = 2^{\nu-1}\frac{\Gamma(\nu)}{c^{\nu}}\lim_{x_0\to 0}\left(x_0^{\mu-\sigma\nu}\right) = \begin{cases} 0, & \mu > \sigma\nu \\ 2^{\nu-1}\frac{\Gamma(\nu)}{c^{\nu}}, & \mu = \sigma\nu \\ \infty, & \mu < \sigma\nu \end{cases} \tag{A3}$$

one gets a system of to equations for A_1 and A_2. We note that continuity of the derivative is well-defined only for $\alpha < 1$. For $\alpha \geqslant 1$ the derivatives of $\tilde{Q}_I$ and $\tilde{Q}_{II}$ diverge in the limit $x_0 \to 0$ as we show in turn. To compute the derivatives we need to make use of the properties

$$\frac{\mathrm{d}K_{\nu}(z)}{\mathrm{d}z} = -K_{\nu-1}(z) - \frac{\nu}{z}K_{\nu}(z) \tag{A4}$$

and $K_{-\nu}(z) = K_{\nu}(z)$. The derivatives of $\tilde{Q}$ given in equation (A1) are of the form

$$\left[\frac{\partial \tilde{Q}_{I,II}(p,s|x_0)}{\partial x_0}\right]_{x_0=0} = A_{1,2}\frac{2-\alpha}{2}c\lim_{x_0\to 0}\left[x_0^{\frac{1-\alpha}{2}}K_{\frac{1-\alpha}{2-\alpha}}\left(cx_0^{1-\frac{\alpha}{2}}\right)\right]$$

where c is the coefficient of $x_0^{1-\frac{\alpha}{2}}$ in the arguments of the Bessel functions of equation (A1). When $\alpha < 1$ the parameter ν in (A3) is $\nu = (1-\alpha)/(2-\alpha) > 0$ and $\mu = (1-\alpha)/2$, $\sigma = 1-\alpha/2$. In this case, $\mu = \sigma\nu$ so that

$$\left[\frac{\partial \tilde{Q}_{I,II}(p,s|x_0)}{\partial x_0}\right]_{x_0=0} = A_{1,2}\frac{2-\alpha}{2^{\frac{3-\alpha}{2-\alpha}}}c^{\frac{1}{2-\alpha}}\Gamma\left(\frac{1-\alpha}{2-\alpha}\right),\ \alpha < 1$$

When $\alpha \geqslant 1$ we have $\nu < 0$ but since $K_{\nu}(\cdot) = K_{-\nu}(\cdot)$ the derivative in the limit $x_0 \to 0$ reads

$$\left[\frac{\partial \tilde{Q}_{I,II}(p,s|x_0)}{\partial x_0}\right]_{x_0=0} = A_{1,2}\frac{2-\alpha}{2}c\lim_{x_0\to 0}\left[x_0^{\frac{1-\alpha}{2}}K_{\frac{\alpha-1}{2-\alpha}}\left(cx_0^{1-\frac{\alpha}{2}}\right)\right] = \infty,\ \alpha > 1.$$

Finally, plugging A_1 and B_1 in equation (A1) one finds (36).

J. Stat. Mech. (2026) 013203

Appendix B. Derivation of equation (46)

The solution of (45) for the piecewise diffusion coefficient can be written as

$$\begin{aligned}
\tilde{Q}_I(p,s|x_0) &= \frac{1}{s} + C_1 \mathrm{e}^{x_0\sqrt{\frac{s}{D_-}}},\\
\tilde{Q}_{II}(p,s|x_0) &= \frac{1}{s+p} + C_2 \mathrm{e}^{-x_0\sqrt{\frac{s+p}{D_-}}} + C_3 \mathrm{e}^{x_0\sqrt{\frac{s+p}{D_-}}},\\
\tilde{Q}_{III}(p,s|x_0) &= \frac{1}{s+p} + C_4 \mathrm{e}^{-x_0\sqrt{\frac{s+p}{D_+}}} + C_5 \mathrm{e}^{x_0\sqrt{\frac{s+p}{D_+}}},\\
\tilde{Q}_{IV}(p,s|x_0) &= \frac{1}{s} + C_6 \mathrm{e}^{-x_0\sqrt{\frac{s}{D_+}}},\ x_0 > a.
\end{aligned} \tag{B1}$$

The constants C_i with $i = 1,\ldots,6$ can be found from the matching conditions

$$\begin{aligned}
\tilde{Q}_I(p,s|x_0=-a) &= \tilde{Q}_{II}(p,s|x_0=-a)\\
\tilde{Q}_{II}(p,s|x_0=0) &= \tilde{Q}_{III}(p,s|x_0=0)\\
\tilde{Q}_{III}(p,s|x_0=a) &= \tilde{Q}_{IV}(p,s|x_0=a)\\
\left[\frac{\partial\tilde{Q}_I(p,s|x_0)}{\partial x_0}\right]_{x_0=-a} &= \left[\frac{\partial\tilde{Q}_{II}(p,s|x_0)}{\partial x_0}\right]_{x_0=-a}\\
\left[\frac{\partial\tilde{Q}_{II}(p,s|x_0)}{\partial x_0}\right]_{x_0=0} &= \left[\frac{\partial\tilde{Q}_{III}(p,s|x_0)}{\partial x_0}\right]_{x_0=0}\\
\left[\frac{\partial\tilde{Q}_{III}(p,s|x_0)}{\partial x_0}\right]_{x_0=a} &= \left[\frac{\partial\tilde{Q}_{IV}(p,s|x_0)}{\partial x_0}\right]_{x_0=a}.
\end{aligned} \tag{B2}$$

Solving the system of algebraic equations for C_i we finally obtain the solution for the characteristic equation given by equation (46).

Appendix C. Derivation of equation (53)

Following the same procedure as in appendix A, the solution of equation (45) for the power law diffusion coefficient (9) is given by

$$\begin{aligned}
\tilde{Q}_I(p,s|x_0) &= \frac{1}{s} + A_1|x_0|^{1/2} K_{\frac{1}{2-\alpha}}\left(\frac{2}{2-\alpha}|x_0|^{1-\frac{\alpha}{2}}\sqrt{\frac{s}{D_0}}\right),\\
\tilde{Q}_{II}(p,s|x_0) &= \frac{1}{s+p} + A_2|x_0|^{1/2} K_{\frac{1}{2-\alpha}}\left(\frac{2}{2-\alpha}|x_0|^{1-\frac{\alpha}{2}}\sqrt{\frac{s+p}{D_0}}\right)\\
&\quad + A_3|x_0|^{1/2} I_{\frac{1}{2-\alpha}}\left(\frac{2}{2-\alpha}|x_0|^{1-\frac{\alpha}{2}}\sqrt{\frac{s+p}{D_0}}\right),
\end{aligned}$$

J. Stat. Mech. (2026) 013203

$$\tilde{Q}_{III}(p,s|x_0) = \frac{1}{s+p} + A_4 x_0^{1/2} K_{\frac{1}{2-\alpha}}\left(\frac{2}{2-\alpha} x_0^{1-\frac{\alpha}{2}} \sqrt{\frac{s+p}{D_0}}\right) + A_5 x_0^{1/2} I_{\frac{1}{2-\alpha}}\left(\frac{2}{2-\alpha} x_0^{1-\frac{\alpha}{2}} \sqrt{\frac{s+p}{D_0}}\right),$$
$$\tilde{Q}_{IV}(p,s|x_0) = \frac{1}{s} + A_6 x_0^{1/2} |K_{\frac{1}{2-\alpha}}\left(\frac{2}{2-\alpha} x_0^{1-\frac{\alpha}{2}} \sqrt{\frac{s}{D_0}}\right). \tag{C1}$$

The constant A_i with $i = 1,\ldots,6$ can be found using the matching conditions (B2). At the boundary $x_0 = 0$ we employ the property (A3). The system of equations for the constants is

$$A_2\varphi(s+p,a) + A_3\phi(s+p,a) - A_1\varphi(s,a) = \frac{p}{s(s+p)}$$
$$A_4\varphi(s+p,a) + A_5\phi(s+p,a) - A_6\varphi(s,a) = \frac{p}{s(s+p)}$$

$A_2 = A_4$

$$A_1\left[\frac{\mathrm{d}\varphi(s,x_0)}{\mathrm{d}x_0}\right]_{x_0=a} = A_2\left[\frac{\mathrm{d}\varphi(s+p,x_0)}{\mathrm{d}x_0}\right]_{x_0=a} + A_3\left[\frac{\mathrm{d}\phi(s+p,x_0)}{\mathrm{d}x_0}\right]_{x_0=a}$$
$$\times (A_2+A_4)\left[\frac{\mathrm{d}\varphi(s+p,x_0)}{\mathrm{d}x_0}\right]_{x_0=0} + (A_3+A_5)\left[\frac{\mathrm{d}\phi(s+p,x_0)}{\mathrm{d}x_0}\right]_{x_0=0} = 0$$
$$\times A_4\left[\frac{\mathrm{d}\varphi(s+p,x_0)}{\mathrm{d}x_0}\right]_{x_0=a} + A_5\left[\frac{\mathrm{d}\phi(s+p,x_0)}{\mathrm{d}x_0}\right]_{x_0=a} = A_6\left[\frac{\mathrm{d}\varphi(s,x_0)}{\mathrm{d}x_0}\right]_{x_0=a} \tag{C2}$$

where we have defined the functions

$$\varphi(s,x_0) = \sqrt{x_0} K_{\frac{1}{2-\alpha}}\left(\frac{2}{2-\alpha} x_0^{1-\frac{\alpha}{2}} \sqrt{\frac{s}{D_0}}\right)$$
$$\phi(s,x_0) = \sqrt{x_0} I_{\frac{1}{2-\alpha}}\left(\frac{2}{2-\alpha} x_0^{1-\frac{\alpha}{2}} \sqrt{\frac{s}{D_0}}\right). \tag{C3}$$

The derivatives in equations (C2) evaluated at $x_0 = 0$ are divergent unless $\alpha < 1$. Computing the derivatives using the properties of the Bessel functions using (A4) and evaluating them at the boundaries $x_0 = 0$ and $x_0 = a$ we solve the system of equations for the constants and find

$$\tilde{Q}(p,s|0) = \frac{1}{s+p}\left[1 + \frac{p}{s}\frac{\mathcal{H}_1(s,p)}{\mathcal{H}_2(s,p)}\right] \tag{C4}$$

after setting $x_0 = 0$. The functions $\mathcal{H}_1(s,p)$ and $\mathcal{H}_2(s,p)$ are

$$\mathcal{H}_1(s,p) = \frac{\Gamma\left(\frac{1}{2-\alpha}\right)}{2\left(\frac{a^{1-\frac{\alpha}{2}}}{2-\alpha}\sqrt{\frac{s+p}{D_0}}\right)^{\frac{1}{2-\alpha}}} \quad \text{and} \quad \mathcal{H}_2(s,p) = \psi_1 - \psi_2\psi_3 \tag{C5}$$

J. Stat. Mech. (2026) 013203

where

$$\begin{aligned}
\psi_1 &= K_{\frac{1}{2-\alpha}}\left(\frac{2}{2-\alpha}a^{1-\frac{\alpha}{2}}\sqrt{\frac{s+p}{D_0}}\right)+\sigma_\alpha I_{\frac{1}{2-\alpha}}\left(\frac{2}{2-\alpha}a^{1-\frac{\alpha}{2}}\sqrt{\frac{s+p}{D_0}}\right)\\
\psi_2 &= \frac{2}{2-\alpha}a^{1-\frac{\alpha}{2}}\sqrt{\frac{s+p}{D_0}}\left[K_{\frac{1-\alpha}{2-\alpha}}\left(\frac{2}{2-\alpha}a^{1-\frac{\alpha}{2}}\sqrt{\frac{s+p}{D_0}}\right)\right.\\
&\quad\left.-\sigma_\alpha I_{\frac{3-\alpha}{2-\alpha}}\left(\frac{2}{2-\alpha}a^{1-\frac{\alpha}{2}}\sqrt{\frac{s+p}{D_0}}\right)\right]-\frac{2\sigma_\alpha}{2-\alpha}I_{\frac{1}{2-\alpha}}\left(\frac{2}{2-\alpha}a^{1-\frac{\alpha}{2}}\sqrt{\frac{s+p}{D_0}}\right)\\
\psi_3 &= \frac{K_{\frac{1}{2-\alpha}}\left(\frac{2}{2-\alpha}a^{1-\frac{\alpha}{2}}\sqrt{\frac{s}{D_0}}\right)}{\frac{2}{2-\alpha}a^{1-\frac{\alpha}{2}}\sqrt{\frac{s}{D_0}}K_{\frac{1-\alpha}{2-\alpha}}\left(\frac{2}{2-\alpha}a^{1-\frac{\alpha}{2}}\sqrt{\frac{s}{D_0}}\right)}
\end{aligned}\tag{C6}$$

and

$$\sigma_\alpha = \frac{\pi/2}{\sin\left(\pi\frac{1-\alpha}{2-\alpha}\right)}.$$

Before proceeding to perform the double Laplace inversion we consider the long time limit for which we consider s and p very small and comparable. In this limit, the arguments of the Bessel functions in equation (C6) are small and to approximate ψ_1 and ψ_3 we can make use of (A3) and

$$I_\nu(z) \simeq \frac{1}{\Gamma(1+\nu)}\left(\frac{z}{2}\right)^\nu \quad \text{as} \quad z\to 0.$$

However, to approximate ψ_2 we need to go to the next order in the expansion of $K_\nu(\cdot)$ for small argument so that we have to consider

$$K_\nu(z) \simeq \frac{\Gamma(\nu)\Gamma(1-\nu)}{2}\left[\frac{1}{\Gamma(1-\nu)}\left(\frac{z}{2}\right)^{-\nu}-\frac{1}{\Gamma(1+\nu)}\left(\frac{z}{2}\right)^{\nu}\right]$$

for $\nu<1$. Under these considerations we find

$$\begin{aligned}
\psi_1 &\simeq \frac{1}{2}\Gamma\left(\frac{1}{2-\alpha}\right)\left(\frac{a^{1-\frac{\alpha}{2}}}{2-\alpha}\sqrt{\frac{s+p}{D_0}}\right)^{-\frac{1}{2-\alpha}}\\
\psi_2 &\simeq -\frac{2-\alpha}{1-\alpha}\Gamma\left(\frac{1}{2-\alpha}\right)\left(\frac{a^{1-\frac{\alpha}{2}}}{2-\alpha}\sqrt{\frac{s+p}{D_0}}\right)^{\frac{3-2\alpha}{2-\alpha}}\\
\psi_3 &\simeq \frac{\Gamma\left(\frac{1}{2-\alpha}\right)}{2\Gamma\left(\frac{1-\alpha}{2-\alpha}\right)}\left(\frac{a^{1-\frac{\alpha}{2}}}{2-\alpha}\sqrt{\frac{s}{D_0}}\right)^{-\frac{2}{2-\alpha}}
\end{aligned}$$

and finally, from (C4) we find the expression for the characteristic function (53) in the long time limit for both T_a and t.

J. Stat. Mech. (2026) 013203

References

[1] Lançon P, Batrouni G, Lobry L and Ostrowsky N 2001 Drift without flux: Brownian walker with a space-dependent diffusion coefficient *Europhys. Lett.* **54** 28

[2] Yang M and Ripoll M 2012 Drift velocity in non-isothermal inhomogeneous systems *J. Chem. Phys.* **136** 204508

[3] Maris J J E, Fu D, Meirer F and Weckhuysen B M 2021 Single-molecule observation of diffusion and catalysis in nanoporous solids *Adsorption* **27** 423

[4] Mittal J, Truskett T M, Errington J R and Hummer G 2008 Layering and position-dependent diffusive dynamics of confined fluids *Phys. Rev. Lett.* **100** 145901

[5] Cherstvy A G and Metzler R 2013 Population splitting, trapping and non-ergodicity in heterogeneous diffusion processes *Phys. Chem. Chem. Phys.* **15** 20220

[6] Cherstvy A G, Chechkin A V and Metzler R 2013 Anomalous diffusion and ergodicity breaking in heterogeneous diffusion processes *New J. Phys.* **15** 083039

[7] Manzo C and Garcia-Parajo M F 2015 A review of progress in single particle tracking: from methods to biophysical insights *Rep. Prog. Phys.* **78** 124601

[8] Weron A, Burnecki K, Akin E J, Solé L, Balcerek M, Tamkun M M and Krapf D 2017 Ergodicity breaking on the neuronal surface emerges from random switching between diffusive states *Sci. Rep.* **7** 5404

[9] Norregaard K, Metzler R, Ritter C M, Berg-S Ørensen K and Oddershede L B 2017 Manipulation and motion of organelles and single molecules in living cells *Chem. Rev.* **117** 4342

[10] Chechkin A V, Seno F, Metzler R and Sokolov I M 2017 Brownian yet non-Gaussian diffusion: from superstatistics to subordination of diffusing diffusivities *Phys. Rev. X* **7** 021002

[11] Krapf D and Metzler R 2019 Strange interfacial molecular dynamics *Phys. Today* **72** 48

[12] Kühn T, Ihalainen T O, Hyväluoma J, Dross N, Willman S F, Langowski J and Vihinen-Ranta M 2011 Protein diffusion in mammalian cell cytoplasm *PLoS One* **6**

[13] English B P, Hauryliuk V, Sanamrad A, Tankov S, Dekker N H and Elf J 2011 Single-molecule investigations of the stringent response machinery in living bacterial cells *Proc. Natl Acad. Sci. USA* **108** E365

[14] Richardson L F 1926 Atmospheric diffusion shown on a distance-neighbour graph *Proc. R. Soc. A* **110** 709

[15] Dentz M, Gouze P, Russian A, Dweik J and Delay F 2012 Diffusion and trapping in heterogeneous media: an inhomogeneous continuous time random walk approach *Adv. Water Resour.* **49** 13

[16] Loverdo C, Bénichou O, Voituriez R, Biebricher A, Bonnet I and Desbiolles P 2009 Quantifying hopping and jumping in facilitated diffusion of DNA-binding proteins *Phys. Rev. Lett.* **102** 188101

[17] Cherstvy A G, Chechkin A V and Metzler R 2014 Particle invasion, survival and non-ergodicity in 2D diffusion processes with space-dependent diffusivity *Soft Matter* **10** 1591

[18] Wang X, Deng W and Chen Y 2019 Ergodic properties of heterogeneous diffusion processes in a potential well *J. Chem. Phys.* **150** 164121

[19] Leibovich N and Barkai E 2019 Infinite ergodic theory for heterogeneous diffusion processes *Phys. Rev. E* **99** 042138

[20] West B, Bulsara A, Lindenberg K, Seshadri V and Shuler K 1979 Stochastic processes with non-additive fluctuations: I. Itô and Stratonovich calculus and the effects of correlations *Physica A* **97** 211

[21] Fa K S 2005 Exact solution of the Fokker-Planck equation for a broad class of diffusion coefficients *Phys. Rev. E* **72** 020101

[22] Dupont T, Giordano S, Cleri F and Blossey R 2024 Short-time expansion of one-dimensional Fokker-Planck equations with heterogeneous diffusion *Phys. Rev. E* **109** 064106

[23] Pešek J, Baerts P, Smeets B, Maes C and Ramon H 2016 Mathematical model suitable for efficient simulation of thin semi-flexible polymers in complex environments *Soft Matter* **12** 3360

[24] Regev S, GrØnbech-Jensen N and Farago O 2016 Isothermal Langevin dynamics in systems with power-law spatially dependent friction *Phys. Rev. E* **94** 012116

[25] Gardiner C W 2004 Handbook of stochastic methods for physics, chemistry and the natural sciences *Series Springer Series in Synergetics* vol 13, 3rd edn (Springer) p xviii+415

[26] Bardou F, Bouchaud J-P, Aspect A and Cohen-Tannoudji C 2001 *Lévy Statistics and Laser Cooling: How Rare Events Bring Atoms to Rest* (Cambridge University Press)

[27] Farago O and Gr Ønbech-Jensen N 2016 On the connection between dissipative particle dynamics and the itô-stratonovich dilemma *J. Chem. Phys.* **144** 084102

[28] Bray A J 2000 Random walks in logarithmic and power-law potentials, nonuniversal persistence and vortex dynamics in the two-dimensional XY model *Phys. Rev. E* **62** 103

J. Stat. Mech. (2026) 013203

[29] Pieprzyk S, Heyes D M and Brańka A C 2016 Spatially dependent diffusion coefficient as a model for ph sensitive microgel particles in microchannels *Biomicrofluidics* **10** 054118
[30] Berezhkovskii A M and Makarov D E 2017 Communication: coordinate-dependent diffusivity from single molecule trajectories *J. Chem. Phys.* **147** 201102
[31] Kaulakys B and Alaburda M 2009 Modeling scaled processes and $1/f^{\beta}$ noise using nonlinear stochastic differential equations *J. Stat. Mech.* 02051
[32] Wang X, Chen Y and Deng W 2018 Feynman-Kac equation revisited *Phys. Rev. E* **98** 052114
[33] Srokowski T 2007 Non-markovian lévy diffusion in nonhomogeneous media *Phys. Rev. E* **75** 051105
[34] Radice M 2023 First-passage functionals of Brownian motion in logarithmic potentials and heterogeneous diffusion *Phys. Rev. E* **108** 044151
[35] Singh P 2022 Extreme value statistics and arcsine laws for heterogeneous diffusion processes *Phys. Rev. E* **105** 024113
[36] Metzler R, Jeon J-H, Cherstvy A G and Barkai E 2014 Anomalous diffusion models and their properties: non-stationarity, non-ergodicity and ageing at the centenary of single particle tracking *Phys. Chem. Chem. Phys.* **16** 24128
[37] Bressloff P C and Lawley S D 2017 Temporal disorder as a mechanism for spatially heterogeneous diffusion *Phys. Rev. E* **95** 060101
[38] Pacheco-Pozo A, Balcerek M, Wyłomanska A, Burnecki K, Sokolov I M and Krapf D 2024 Langevin equation in heterogeneous landscapes: how to choose the interpretation *Phys. Rev. Lett.* **133** 067102
[39] van Milligen B P, Bons P D, Carreras B A and Sanchez R 2005 On the applicability of Fick's law to diffusion in inhomogeneous systems *Eur. J. Phys.* **26** 913
[40] Majumdar S N 2005 Brownian functionals in physics and computer science *Curr. Sci.* **89** 2076
[41] Godreche C and Luck J M 2001 Statistics of the occupation time of renewal processes *J. Stat. Phys.* **104** 489–524
[42] Barkai E 2006 Residence time statistics for normal and fractional diffusion in a force field *J. Stat. Phys.* **123** 883
[43] Lévy P 1940 Sur certains processus stochastiques homogènes *Compositio Math.* **7** 283
[44] Carmi S, Turgeman L and Barkai E 2010 On distributions of functionals of anomalous diffusion paths *J. Stat. Phys.* **141** 1071
[45] Lamperti J 1958 An occupation time theorem for a class of stochastic processes *Trans. Am. Math. Soc.* **88** 380
[46] Méndez V and Flaquer-Galmés R 2025 Statistical properties of stochastic functionals under general resetting *Phys. Rev. E* **112** 044123
[47] Carmi S and Barkai E 2011 Fractional Feynman-Kac equation for weak ergodicity breaking *Phys. Rev. E* **84** 061104
[48] Burov S and Barkai E 2011 Residence time statistics for n renewal processes *Phys. Rev. Lett.* **107** 170601
[49] Yan H and Chen H 2023 Breakdown of arcsine law for resetting Brownian motion *Phys. Scr.* **98** 125226
[50] Barkai E, Flaquer-Galmés R and Méndez V 2023 Ergodic properties of Brownian motion under stochastic resetting *Phys. Rev. E* **108** 064102
[51] Bonetto F, Lebowitz J L and Lukkarinen J 2004 Fourier's law for a harmonic crystal with self-consistent stochastic reservoirs *J. Stat. Phys.* **116** 783
[52] Gradshteyn I S, Ryzhik I M, Zwillinger D and Moll V 2015 *Table of Integrals, Series and Products* (Academic)

J. Stat. Mech. (2026) 013203